UC Riverside
UC Riverside Previously Published Works

Title

The multifunctional autophagy pathway in the human malaria parasite, Plasmodium falciparum

Permalink

Journal

ISSN

Authors

Cervantes, Serena
Bunnik, Evelien M
Saraf, Anita
et al.

Publication Date

DOI

Copyright Information

Peer reviewed

The multifunctional autophagy pathway in the human malaria parasite, *Plasmodium falciparum*

Serena Cervantes,[1,2] Evelien M Bunnik,[2] Anita Saraf,[3] Christopher M Conner,[2] Aster Escalante,[2] Mihaela E Sardiu,[3] Nadia Ponts,[2] Jacques Prudhomme,[2] Laurence Florens,[3] and Karine G Le Roch[2,*]

[1]Graduate Program in Cell, Molecular, and Developmental Biology; University of California, Riverside; Riverside, CA USA; [2]Department of Cell Biology and Neuroscience; University of California, Riverside; Riverside, CA USA; [3]Stowers Institute for Medical Research; Kansas City, MO USA

Autophagy is a catabolic pathway typically induced by nutrient starvation to recycle amino acids, but can also function in removing damaged organelles. In addition, this pathway plays a key role in eukaryotic development. To date, not much is known about the role of autophagy in apicomplexan parasites and more specifically in the human malaria parasite *Plasmodium falciparum*. Comparative genomic analysis has uncovered some, but not all, orthologs of autophagy-related (*ATG*) genes in the malaria parasite genome. Here, using a genome-wide in silico analysis, we confirmed that *ATG* genes whose products are required for vesicle expansion and completion are present, while genes involved in induction of autophagy and cargo packaging are mostly absent. We subsequently focused on the molecular and cellular function of *P. falciparum* ATG8 (PfATG8), an autophagosome membrane marker and key component of the autophagy pathway, throughout the parasite asexual and sexual erythrocytic stages. In this context, we showed that PfATG8 has a distinct and atypical role in parasite development. PfATG8 localized in the apicoplast and in vesicles throughout the cytosol during parasite development. Immunofluorescence assays of PfATG8 in apicoplast-minus parasites suggest that PfATG8 is involved in apicoplast biogenesis. Furthermore, treatment of parasite cultures with bafilomycin A₁ and chloroquine, both lysosomotropic agents that inhibit autophagosome and lysosome fusion, resulted in dramatic morphological changes of the apicoplast, and parasite death. Furthermore, deep proteomic analysis of components associated with PfATG8 indicated that it may possibly be involved in ribophagy and piecemeal microautophagy of the nucleus. Collectively, our data revealed the importance and specificity of the autophagy pathway in the malaria parasite and offer potential novel therapeutic strategies.

Introduction

Malaria continues to be a major global health problem with up to a million deaths per year.[1] The human malaria parasite has a complex life cycle consisting of 3 major stages in the mosquito, the human liver, and the human blood. In the blood stage, merozoites invade erythrocytes and within 48 h the parasite progresses through ring, trophozoite, and schizont stages to produce up to 32 new daughter cells that egress and reinvade new red blood cells. This asexual cycle continues until the human host is stressed. Parasites then undergo gametocytogenesis, which can require up to 2 wk for full differentiation. When another female mosquito takes a blood meal, mature male and female gametocytes are taken up and undergo sexual reproduction in the mosquito midgut to complete the cycle. Throughout its life cycle, the parasite undergoes cell differentiation and metamorphosis multiple times, requiring degradation of unnecessary stage-specific proteins and organelles within host cells. In the

face of increased resistance of *P. falciparum* to current antimalarials, understanding the mechanisms that control the parasite degradation pathways may open new doors for the development of novel antimalarial drugs.

In eukaryotic cells, the autophagosome-lysosome pathway is involved in degradation and recycling of proteins and organelles. Similar to the ubiquitin-proteasome system that degrades short-lived and misfolded proteins,[2] the autophagy pathway consists of a number of sequential steps: selection and tagging of cargo, recognition and transport to proteolytic machinery, degradation of cargo, and recycling of small polypeptides or amino acids. Proteins and organelles targeted for degradation are enveloped by a double membrane to form an autophagosome that fuses with a lysosome to degrade the cargo. There are 3 main membrane-mediated processes conserved through most eukaryotes: 1) macroautophagy (referred to as autophagy hereafter) removes unnecessary proteins and damaged organelles, 2) microautophagy occurs when the lysosome directly envelops cytoplasmic

material, and 3) chaperone-mediated autophagy (CMA) relies on a chaperone protein to translocate individual unfolded proteins into the lysosome. Once thought to be a nonspecific molecular process that recycles proteins for survival under nutrient-limited conditions, autophagy is involved in aging, degradation of pathogens, cell differentiation, and removal of old or damaged organelles.[3]

More than 30 autophagy-related (*ATG*) genes were first discovered in yeast,[4] and were thought to be generally conserved in eukaryotes.[5] However, preliminary data show that the canonical machinery of autophagy in parasitic protists has become diverse as a possible consequence of their adaptive life cycles.[6] *ATG* genes have been modified, lost or have expanded, but, overall, autophagy seems to play a critical role in parasite development.[7] For example, in *Toxoplasma gondii,* an apicomplexan parasite related to *Plasmodium*, orthologs of the ATG12–ATG5 conjugation system have not yet been identified. However, the ATG8 conjugation system has been detected and ATG1 and TOR orthologs have been found to mediate autophagosome formation upon starvation.[8] In addition, it was recently found that in *Toxoplasma*, TgATG3, an E2 conjugating enzyme for the LC3 lipidation process, is essential for regulating mitochondrial homeostasis during tachyzoite development.[9] In the murine rodent malaria parasite, *P. berghei,* autophagy is required to remove unnecessary organelles during metamorphosis of the sporozoite into merozoites in hepatocytes.[10]

Despite the publication of these recent studies, not much is known about the role of autophagy in the human malaria parasite, *P. falciparum.* Genome-wide analyses using BLAST searches for either homologs or putative orthologs of known autophagy components have uncovered a rudimentary set of *ATG* genes. Recently, PfATG8, a marker of the phagophore and autophagosome membranes, was shown to localize in the apicoplast membrane at the late schizont and merozoite stages.[11] In the rodent malaria, *P. berghei,* the function of PbATG8 seems restricted to apicoplast biogenesis in the liver stage.[12] The apicoplast is a plastid of secondary endosymbiotic origin that is essential to parasite survival.[13] The role and function of PfATG8 in the apicoplast remains ambiguous, but it has been implied that PfATG8 may be part of endoplasmic reticulum (ER)-related organelle biogenesis, which includes apicoplast membrane biogenesis.[14] In this study, we used a combination of genomic, molecular, cellular, and proteomic approaches to further investigate the role of *ATG* genes throughout the *P. falciparum* asexual and sexual blood stages. We demonstrated that the human malaria parasite has modified the canonical autophagy pathway to a rudimentary set of *ATG* genes that participate not only in apicoplast biogenesis, but in additional functions of cellular development.

Results

Identification of autophagy genes in *P. falciparum*

Previous in silico analysis of *P. falciparum's* genome using BLAST retrieved few homologs of *ATG* genes.[6,11] To uncover a complete list of *ATG* genes in *P. falciparum,* we conducted a hidden Markov model (HMM) search for ATG protein domains.

The HMM methodology has a high sensitivity for the detection of less conserved regions, and is therefore better applicable to apicomplexan parasites which seem to have modified the canonical autophagy pathway.[15]

Of the upstream autophagy pathway, none of the members of the Atg1 kinase complex functional unit were detected, even though putative Atg1 and Atg17 orthologs have been reported previously (**Table S1**).[16] Likewise, the transmembrane protein Atg9 was not identified. However, we detected potential candidates for PfATG6 and PfATG14, members of the class III PtdIns 3-kinase complex. In addition, a possible PfATG2 candidate with homology in the C-terminal region was identified.[17] Altogether, this in silico study suggests that the human malaria parasite lacks proteins critical for detection of nutrient limitation and induction of the canonical autophagy pathway, unlike higher eukaryotes and the apicomplexan *T. gondii.*

Of the downstream pathway, we identified most genes in the Atg12 conjugation system with the exception of the E2-like enzyme Atg10 (**Table S1**). In addition, all members of the Atg8 conjugation system (Atg7, Atg3, and Atg4) were detected. Finally, a homolog of the lipase Atg15, responsible for breakdown of intravacuolar membranes, was identified.[18] As a whole, our comparative genomics analysis has expanded the *ATG* gene list found in *P. falciparum* and indicates that a rudimentary autophagy pathway is present and likely functional.

PfATG8 and GFP-PfATG8 expression and localization during the asexual erythrocytic stage

To investigate the role of autophagy in the human malaria parasite at the molecular and cellular levels, we first explored the role of ATG8 during the erythrocytic cycle. ATG8 is the standard autophagosome marker and is essential to autophagosome formation. It remains present on the outer autophagosome membrane until, or just before, fusion with the lysosome, and a population of ATG8 also remains bound to the inner autophagosome membrane.[19] We generated a custom PfATG8-specific antibody and analyzed PfATG8 protein expression in ring, trophozoite, and schizont stage parasites. Protein concentrations of parasite lysates from each stage were determined by Bradford assay[20] and equal amounts of protein were resolved by SDS-PAGE and ponceau staining (**Fig. S1A**). PfATG8 expression was detected at all stages of the asexual cycle, with a decreased abundance at the trophozoite stage (**Fig. 1A**; **Fig. S1A**). Similar to previous reports that suggest PfATG8 is primarily present in a phosphatidylethanolamine (PE)-conjugated form,[11] we observed PfATG8 as a single band (**Fig. 1A**; **Fig. S1A**). In most other eukaryotes, ATG8 requires cleavage by ATG4 to expose a glycine for conjugation to PE. In contrast, the terminal residue of PfATG8 is a glycine and we therefore speculate that it is predominately lipidated during the asexual cycle.

Subcellular fractions of mixed-stage parasites were immunoblotted for PfATG8. Examination of cytoplasmic, nuclear, and membrane fractions in the 3D7 cell line indicated that PfATG8 was predominantly incorporated into membranes (**Fig. 1B**; **Fig. S1B**). To validate our fractionation, we used the ACP$_{transit}$-GFP cell line, which expresses GFP in the cytosol, as a blotting control for the cytosolic fraction (GFP) and the nuclear fraction
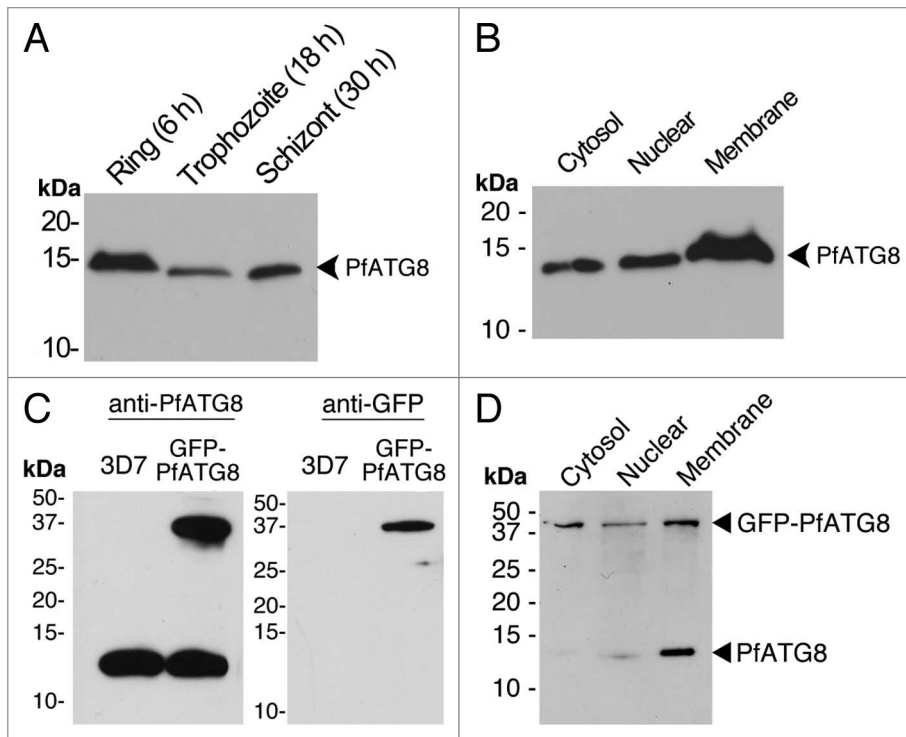
Figure 1. Expression of PfATG8 throughout the erythrocytic cycle. (**A**) Immunoblot analysis of PfATG8 expression in tightly synchronized parasites harvested at the ring, trophozoite, and schizont stage. Protein concentration was determined by Bradford analysis and 30 μg of parasite lysate was loaded in each lane. Using a custom-generated anti-PfATG8 antibody, it was observed that PfATG8 protein is present throughout the asexual cycle, albeit at lower abundance in the trophozoite stage. (**B**) Immunoblot analysis showing the expression of endogenous PfATG8 in cytosolic, nuclear, and membrane fractions of parasite lysates. Mixed-stage 3D7 parasite cultures were used for subcellular fractionation. Protein concentration was determined by Bradford assay and 30 μg of protein was loaded for the cytosolic and nuclear fractions, while 10 μg of protein was loaded for the membrane fraction. PfATG8 is detected in all fractions, but is predominantly membrane-bound. (**C**) Immunoblot analysis of the GFP-PfATG8 transiently-transfected *P. falciparum* cell line. Mixed-stage 3D7 and GFP-PfATG8 parasites were lysed and 30 μg of lysate was loaded into each lane. Endogenous PfATG8 was detected using anti-PfATG8 at 14 kDa, while the fusion protein GFP-PfATG8 was detected by both anti-GFP and anti-PfATG8 antibodies at the expected molecular weight of 41 kDa. For all panels, relative amounts of protein loaded were assessed by Ponceau-staining the full-length PVDF membrane prior to blotting (**Fig. S1**). The sizes of molecular mass markers are indicated in kDa.

molecular weight of 47 kDa (**Fig. 1C**; **Fig. S1D**). No apparent difference in GFP-PfATG8 parasite growth rate or propagation was observed, although blood smears of parasites did have an enlarged digestive phagolysosome (food vacuole) phenotype at the trophozoite stage (**Fig. S3B**). The GFP-PfATG8-transfected cell line displayed a similar pattern as compared with anti-PfATG8 labeling with a diffuse GFP signal throughout the cytoplasm (**Fig. S4**). Immunoblot analysis showed that while GFP-PfATG8 was also membrane-bound, GFP-PfATG8 was more abundant than endogenous PfATG8 in cytosolic fractions (**Fig. 1D**; **Fig S1E**). Interestingly, at the trophozoite stage the localization of GFP-PfATG8 and PfATG8 exhibited less overlap than at other stages. Metabolic activity is high during the trophozoite stage and as vesicle transport increases, the exogenous PfATG8 and GFP-PfATG8 may be recycled onto newly synthesized vesicles. PfATG8 was recently reported to be solely localized in the apicoplast during the merozoite stage.[11] However, we observed PfATG8-decorated vesicles, presumably autophagosomes, at all stages of the asexual blood cycle, as recently shown by Tomlins et al.[21]

PfATG8 vesicles and localization with the apicoplast

The transgenic D10 strain with the apicoplast acyl carrier protein (ACP) fused to GFP was used to confirm the possible colocalization of PfATG8 and the apicoplast.[22] PfATG8 was indeed detected close to the apicoplast, suggesting a possible biological role of this protein in the biogenesis of the organelle (**Fig. 2**). However,

(histone H3) (**Fig S1C**). To further define the subcellular localization of PfATG8, synchronized 3D7 parasite cultures were immunolabeled with anti-PfATG8 at all stages of the asexual cell cycle. PfATG8 was found on punctate structures of 200- to 350-nm diameter throughout the asexual cycle (**Fig. S2**). These structures are smaller than the classical autophagosome of 300- to 900-nm diameter and larger than the typical 150-nm diameter cytoplasm-to-vacuole targeting vesicles seen in yeast. During the ring stage, small punctate structures were observed, which merged into a circular structure during the trophozoite stage with additional puncta observed in the cytosol of *P. falciparum* and host red blood cell (RBC; **Fig. S2**). This circular structure branched out as the parasite underwent schizogony, and finally segmented into daughter cells (**Fig. S2**). To complement our results, we generated a GFP-PfATG8 transiently transfected cell line that expresses the fusion protein at the expected

additional small punctate structures that do not completely overlap with the apicoplast were observed throughout the asexual cycle. Quantification of vesicles revealed 1 to 2 puncta at the ring stage, while 10 to 15 puncta, and 15 or more were observed at the trophozoite and the schizont stages, respectively. Moreover, the branching of PfATG8 during the trophozoite and schizont stages covered a larger area than ACP-GFP and appeared bulbous compared with the smooth branching of the apicoplast. In this parasite line, vesicles decorated with PfATG8 were also observed in the host erythrocyte from the late ring to late trophozoite stages.

Recently, it was reported that apicoplast-minus *P. falciparum* strains could be established by treatment of the parasites with antibiotics that inhibit apicoplast gene transcription and translation, followed by rescue of the parasites by isopentenyl pyrophosphate (IPP) supplementation.[23] In antibiotic-treated ACP-GFP parasites rescued with IPP, apicoplast proteins were localized in

Figure 2. PfATG8 immunofluorescence staining throughout the erythrocytic cycle. Tightly synchronized *P. falciparum* D10-ACP-GFP parasites were immunolabeled with anti-PfATG8. D10 parasites express ACP-GFP, an apicoplast signal and transit peptide fused to GFP that localizes to the apicoplast. Localization of ACP-GFP and PfATG8 can be observed, although PfATG8 appears to surround the apicoplast, indicating a possible association with the outer membrane. Additional PfATG8 vesicles can be observed in the cytosol and host red blood cell from the late ring to late trophozoite stage, when parasites are metabolically active. DAPI is used as a DNA marker in blue. Scale bar: 5 μm.
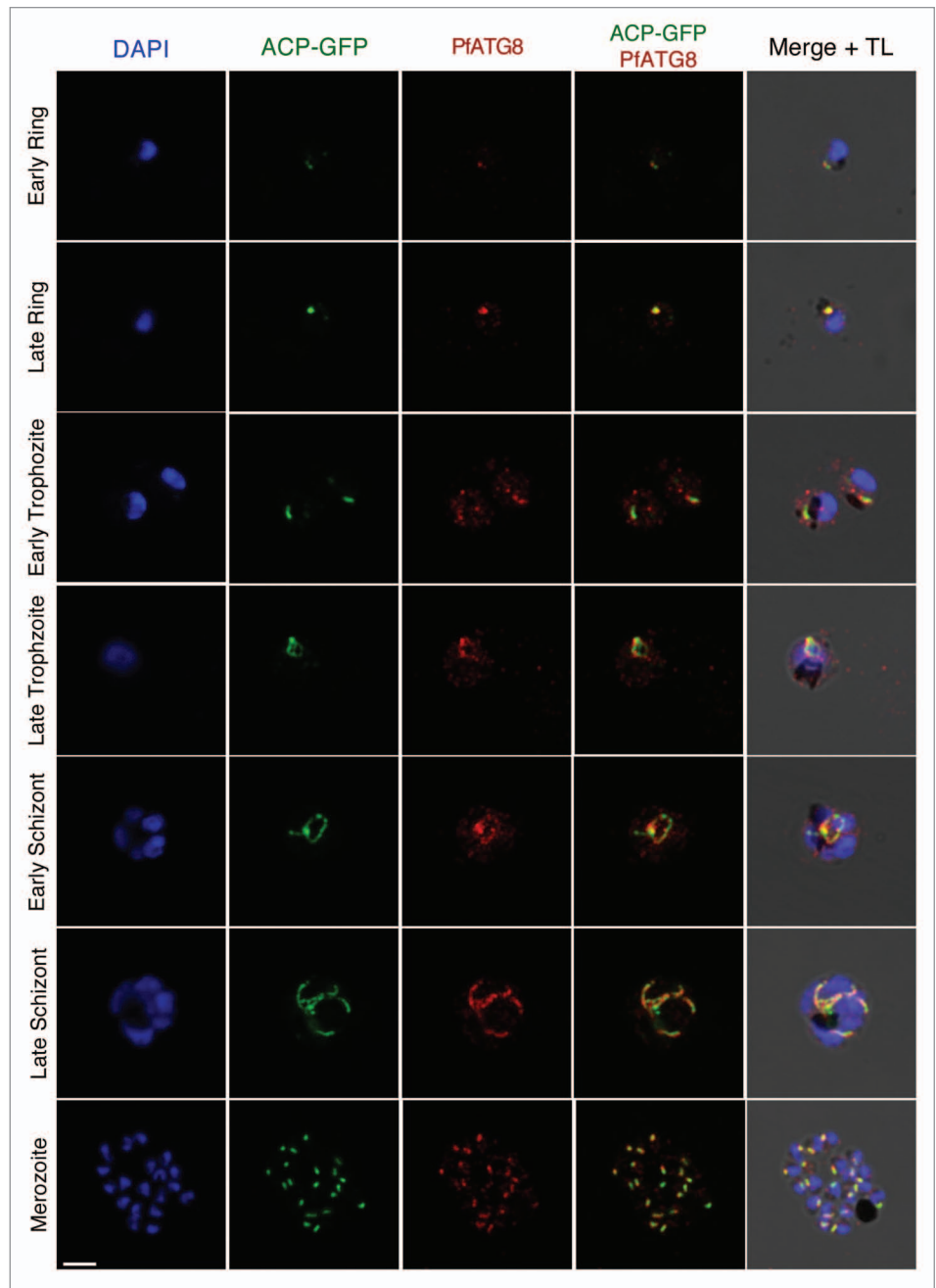

numerous small foci spread throughout the cell with additional diffuse GFP staining, while branching of the apicoplast at the schizont stage was completely abolished. Labeling of apicoplast-minus parasites with PfATG8 showed that PfATG8 vesicles overlap with some, but not all, ACP-GFP vesicles (**Fig. 3**). Quantification of vesicles revealed that two-thirds of PfATG8 vesicles did not overlap with the ACP-GFP foci.

PfATG8 localization during gametogenesis

Next, we investigated the distribution of PfATG8 during the sexual phase of the erythrocytic stage. In contrast to the asexual cycle which is completed within 48 h, differentiation into gametocytes is a relatively slow process requiring 8–10 d.[24] In the NF54 strain, that readily produces gametocytes, the apicoplast ACP-GFP cell line and our newly generated GFP-PfATG8 parasite line, gametocytes of all stages

Figure 3. PfATG8 immunofluorescent staining in apicoplast-minus malaria parasites. The integrity of the apicoplast in these parasites was lost using treatment with the antibiotic chloramphenicol. GFP-ACP parasite cultures were rescued by supplementing media with isopentenyl pyrophosphate (IPP), the essential product from the non-mevalonate isoprenoid precursor pathway in the apicoplast. The large apicoplast PfATG8-labeled branching, as observed in untreated parasites, is disrupted into multiple foci in apicoplast-minus parasites. These foci show colocalization of GFP-ACP and PfATG8 vesicles, although additional PfATG8 vesicles can be observed in the cytosol. DAPI is used as a DNA marker in blue. Scale bar: 2.5 μm.
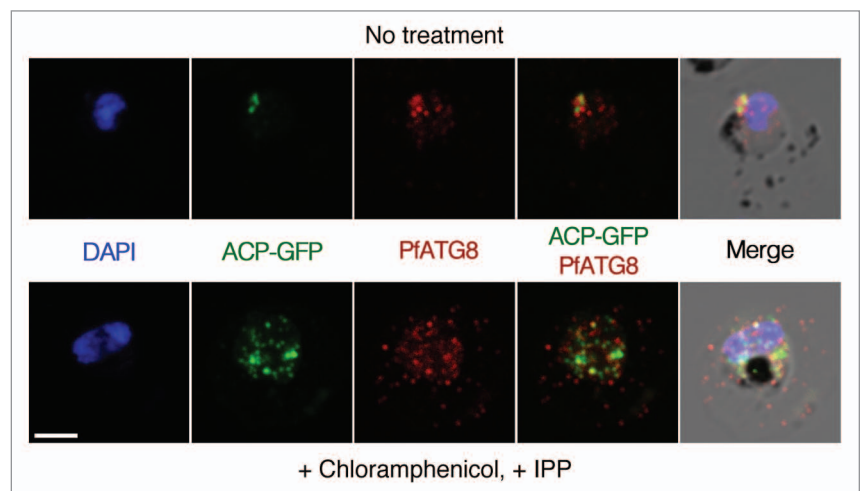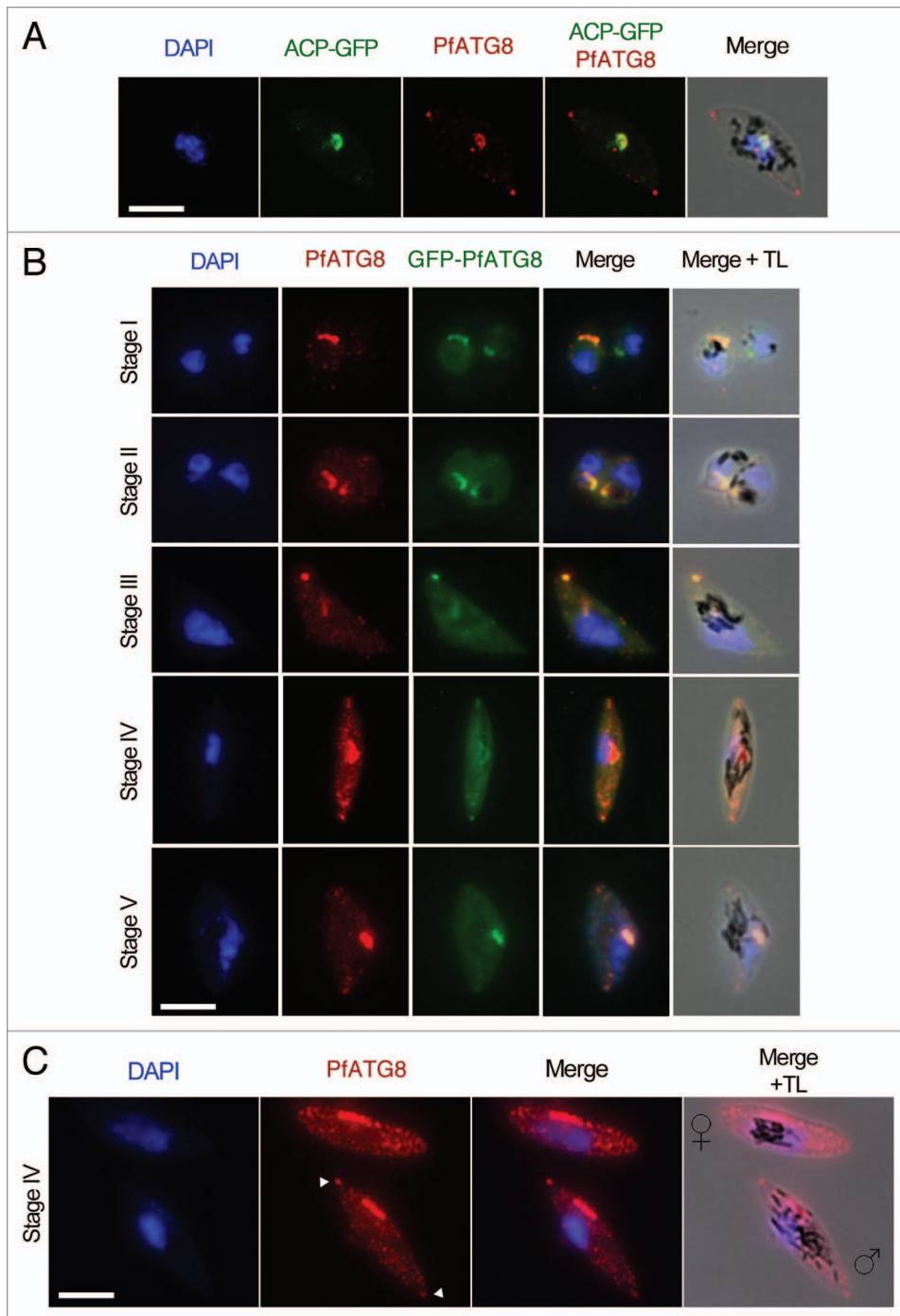
Figure 4. PfATG8 immunofluorescent staining in gametocytes. (**A**) Validation of PfATG8 localization using the ACP-GFP cell line. A clear localization of GFP-PfATG8 and the apicoplast can be observed. (**B**) Expression of PfATG8 in GFP-PfATG8 gametocytes. An abundance of PfATG8-labeled autophagosomes is observed during gametocytogenesis. In stage II-IV, large vesicles are observed at the apical poles. (**C**) Differential PfATG8 pattern in male and female gametocytes. Female NF54 gametocytes at stage IV have rounded poles and PfATG8 vesicles are more uniform in size and distribution in the cytosol, while male gametocytes have larger PfATG8 vesicles at the apical poles (white arrowheads). DAPI is used as a DNA marker in blue. Scale bar: 5 μm.

During stage II–IV, PfATG8 was also present at the apical poles (**Fig. 4B**). Interestingly, the apical pole staining differed depending on the sex of gametocytes. Stage IV male gametocytes displayed a large vesicle at both poles, whereas female gametocytes had vesicles more evenly dispersed outside the nucleus (**Fig. 4C**). Once gametocytes are in the mosquito gut, females will produce a single macrogamete whereas males will produce 8 microgametes. During microgametogenesis, parasites exflagellate and develop axonemes, but the apicoplast and mitochondrion remain in the original gametocyte cytoplasm.[25] A temporal and sex-dependent regulation of the autophagy pathway in male and female gametocytes is therefore not surprising.

Absence of induction of the autophagy pathway by starvation in *P. falciparum*

Autophagy is typically induced by nutrient starvation.[4] However in *P. falciparum*, the *ATG* genes involved in autophagy induction were not detected in our in silico genome-wide analysis (**Table S1**). To validate our in silico data and test whether autophagy could be induced by nutrient limitation in *P. falciparum*, parasite cultures were grown in both serum-free medium and minimal medium devoid of the essential amino acid L-glutamine and serum, with minimal glucose. Ring stage parasites grown in medium without human serum or albumax for 24 h were arrested at the trophozoite stage, and normal growth was restored upon addition of complete medium. A similar state of hibernation has been recently observed in isoleucine-starved parasites.[26] Parasites that were starved for 72 h in minimal medium and then given complete medium produced 1% parasitemia of gametocytes when compared with control parasites. However, despite multiple attempts, incubation in minimal medium for 6, 24, or 72 h

showed numerous PfATG8-associated vesicles throughout the cytosol. In the ACP-GFP cell line, it was observed that PfATG8 localized in the apicoplast adjacent to the nucleus (**Fig. 4A**).

did not increase the amount of PfATG8 autophagosomes (data not shown). These data indicate that unlike other eukaryotic cells, autophagy in the asexual blood stage of *P. falciparum*
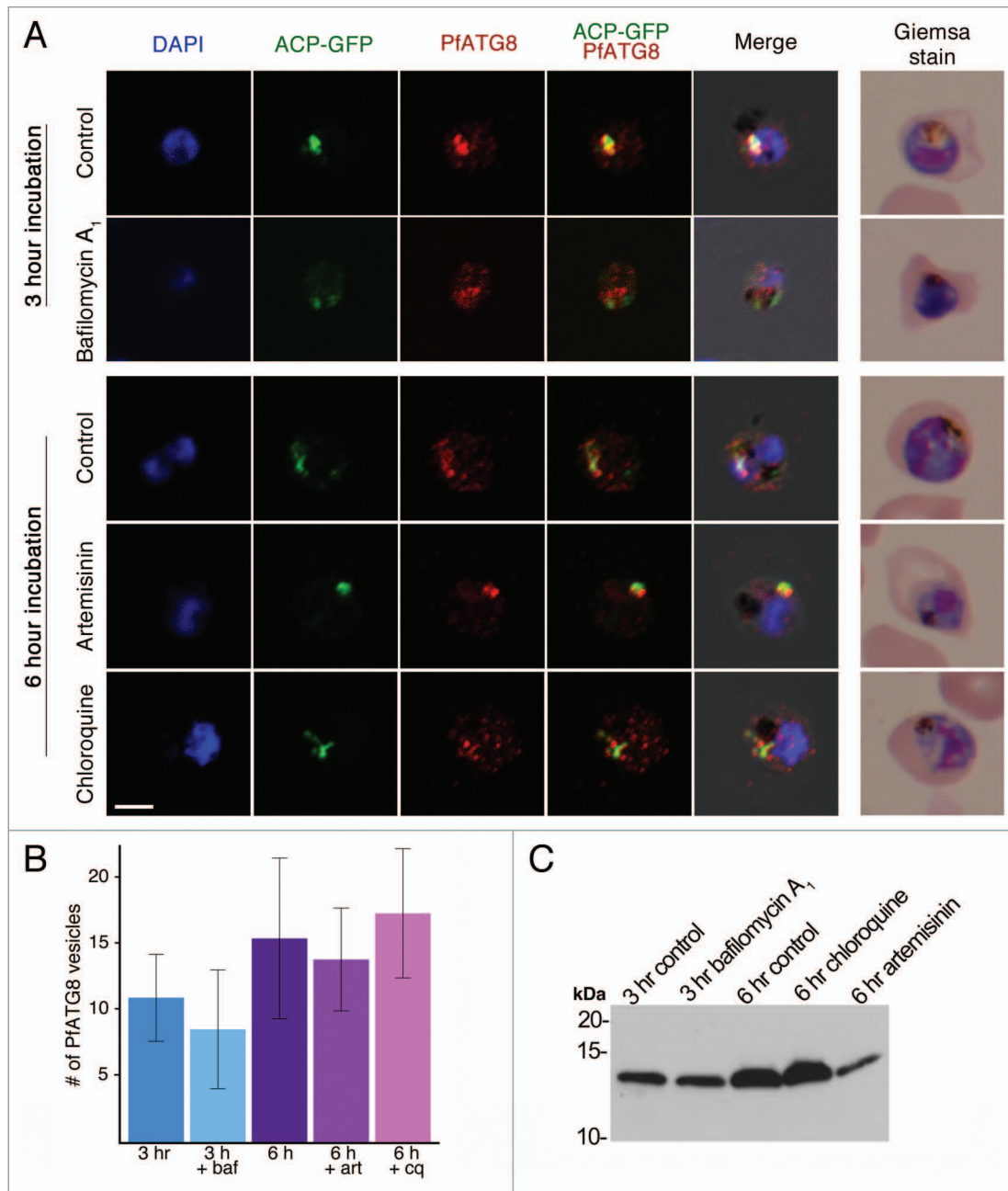
Figure 5. Effect of antimalarial treatment on PfATG8 expression and localization. (**A**) PfATG8 immunofluorescent staining in 3D7 parasites treated with lysosomotropic agents and artemisinin. After 3 h incubation with 75 nM of bafilomycin A_1, branching of the apicoplast is disrupted and multiple PfATG8 autophagosomes can be observed. Artemisinin treatment at a high concentration (25 μM) results in cell cycle progression arrest, and chloroquine treatment, at a concentration of 100 nM (IC_{80}), causes disruption of the apicoplast integrity. DAPI is used as a DNA marker in blue. Scale bar: 2.5 μm. (**B**) Graph of PfATG8 vesicles on trophozoite-stage parasites with or without autophagy inhibitor incubation (baf, 75 nM bafilomycin A_1; art, 25 μM artemisinin; cq, 100 nM chloroquine). (**C**) Western blot analysis of PfATG8 expression levels upon bafilomycin A_1, chloroquine and artemisinin treatment.

cannot be activated under mild starvation conditions, and that parasites starved for long periods of time preferably undergo gametocytogenesis.

Downstream inhibitory effects on *P. falciparum's* autophagy pathway

Traditional methods to induce and inhibit autophagy do not seem to be effective in *P. falciparum*. The lack of classical induction by starvation or drug treatments may be due to the parasite's divergent upstream signaling kinases. Indeed, treatment of parasite cultures with the TOR complex inhibitor rapamycin did not induce autophagy (data not shown), most likely because the parasite lacks a homolog for TOR. Similarly, PfATG8 localization was previously reported to remain unchanged upon treatment of parasites with wortmannin, a PtdIns3K and class I PI3K inhibitor.[11] Both rapamycin and wortmannin work by targeting upstream proteins of the autophagy pathway. Bafilomycin A_1, on the other

hand, is a V-type H^+-ATPase inhibitor that inhibits the downstream fusion events between autophagosomes and lysosomes, and has effects on transport within the endocytic pathway.[27] Here, we observed that bafilomycin A_1 is a potent inhibitor of the chloroquine-sensitive 3D7 strain, and the chloroquine-resistant strains W2 and Dd2, as well as our GFP-PfATG8 cell line, with IC_{50} values ranging between 21 to 26 nM (**Table S2**). The morphological effects of bafilomycin A_1 were examined by treatment of synchronized 3D7 and GFP-PfATG8 parasite cultures at the ring, trophozoite, and schizont stages for 6 and 12 h. A rapid inhibition of parasite growth was observed, in particular at the mature stages (**Fig. S3**). The potent inhibitory effect of bafilomycin A_1 on parasite growth could be reversed by washing bafilomycin A_1 out of the culture medium within 3 h (data not shown). After 3 h of bafilomycin A_1 incubation at 75 nM, early trophozoite parasites decreased in size with a slight decrease of PfATG8-labeled vesicles, from an average of 11 punctate structures to an average of 8.5 puncta (P = 0.005) (**Fig. 5A and B**). This overall decrease of PfATG8 staining was accompanied by dissociation from the apicoplast and an increased staining level in the cytosol. Immunoblot analysis of PfATG8 expression after bafilomycin A_1 treatment did not show a substantial difference when compared with the control (**Fig. 5C**; **Fig. S1F**). Moreover, immunoblot analysis of cytoplasmic and membrane fractions did not indicate changes in subcellular PfATG8 expression (data not shown). Similar to what we observed at the trophozoite stage, schizont-stage parasites incubated with bafilomycin A_1 displayed a strong and significant dissociation between PfATG8 and the apicoplast, and an increase in PfATG8 vesicle staining from an average of 18 to an average of 30 puncta (P = 0.0003) (**Fig. 5A and B**).

In eukaryotic cells, autophagy plays a role in a particular form of cell death. *P. falciparum* was previously reported to undergo vacuolization after 24 h of incubation with antimalarial compounds.[28] We examined the effects of artemisinin, currently the most effective antimalarial agent,[29] and chloroquine on PfATG8 localization. ACP-GFP parasites treated at the trophozoite stage with a high concentration (25 μM) of artemisinin did not show any significant changes in PfATG8 staining pattern (**Fig. 5A**). Parasites did exhibit a delay in cell cycle progression and remained stunted at the trophozoite stage when artemisinin was added (**Fig. 5A**). On the other hand, treatment with chloroquine, which was once the most successful antimalarial drug therapy, but is also often used as a tool to study the autophagy pathway in higher eukaryotes, showed a strong phenotype. In all eukaryotic cells, chloroquine increases the lysosomal pH and prevents the fusion of autophagosomes with lysosomes, and therefore blocks lysosomal protein degradation. Trophozoite parasites treated with 100 nM of chloroquine (IC_{80}) for 6 h displayed fragmentation of the apicoplast with no significant change in PfATG8 vesicles from an average of 15.5 (in the absence of chloroquine) to an average of 17.4 puncta (with chloroquine treatment) (**Fig. 5B**). Whether this phenotype is linked to vesicle traffic inhibition or an active fragmentation process remains to be determined.

Identification of proteins associated with PfATG8

To further confirm the role of the autophagy pathway in parasite development and to identify additional proteins involved in this process, we performed an immunoprecipitation experiment using an anti-GFP antibody on synchronized GFP-PfATG8 cultures in combination with a shotgun mass spectrometry approach. Proteins were identified and quantified using multidimensional protein identification technology (MudPIT) coupled with spectral counting.[30] Parasites of early trophozoite and late schizont stages were either nontreated or were treated with bafilomycin A_1 for 3 h before harvesting to potentially enrich for PfATG8-associated proteins. Proteins were considered positive hits if they passed 2 sets of filtration criteria. First, proteins had to be detected in at least 2 of the 3 technical replicates of at least one sample type, and had to be either not detected in our 2 independent negative controls, or be more than 5-fold enriched compared with these negative controls (a precipitation without the anti-GFP primary antibody, and a GFP-precipitation from the 3D7-HT-GFP cell line that stably expresses GFP in all stages of the parasite life cycle).[31] Second, proteins also had to be detected in at least 4 runs (out of a total of 12 runs) and not in controls, or if detected in controls with a QSpec z-score[32] above 1.7 in at least 1 of the 4 sample types (see Materials and Methods). The lack of significant overlap between proteins from our precipitations and controls validates the strength and specificity of our approach. In total, 101 proteins associated with GFP-PfATG8 vesicles passed our selection criteria (**Table S3**). The autophagy network in human cells undergoing basal autophagy consists of 6 ATG8 orthologs that interact directly with 67 proteins.[33] If the autophagy pathway indeed has multiple functions in the malaria parasite, this number of proteins associating with ATG8 vesicles is not surprisingly high. Evidence for enrichment of PfATG8-associated proteins by bafilomycin A_1 treatment was observed in the schizont stage, where we detected 77 proteins in at least 2 replicates of the treated sample vs. 46 such proteins in the untreated sample. This correlates with an increased amount of PfATG8 vesicles that were observed when parasites were treated with bafilomycin A_1. Among the proteins found to be associated with PfATG8 were PfATG7 (E1-like) and 2 undistinguishable isoforms of PfATG3, whereas PfATG6 was only significantly detected in the drug-treated schizont stage. PfATG2 and PfATG18 were detected in the whole data set, but did not pass our selection criteria, whereas PfATG5 was only detected in one of our controls.

Subsequently, a gene ontology (GO) analysis was performed to find functional enrichments among the proteins associated with PfATG8. A relatively large overlap of significantly enriched GO terms was observed between the different samples (**Fig. S5A**). Among all 101 proteins that were found to be associated with PfATG8, significantly enriched GO terms included those involved in the digestive phagolysosome, the phagolysosome, protein transport, nuclear import, and metabolic processes (**Fig. S5B**; **Table S4**).

In line with the fact that more than half of *P. falciparum*'s proteome is incompletely characterized, approximately one-third of the proteins identified to be associated with PfATG8 were hypothetical proteins. These hypothetical proteins were BLASTed against the yeast genome to find evidence for their function. We found homology of PF3D7_1339700 to the yeast protein Nvj1 that is present

at the formation of nucleus-vacuole junctions and is involved in piecemeal microautophagy of the nucleus.[34-36] In addition, we detected homology of PF3D7_1459000 to yeast Bre5, which is associated with the process of ribophagy.[37,38] Further validation will be required to determine if these homologous proteins are indeed involved in selective autophagy pathways and whether they have a functional role in the human malaria parasite. Collectively, these data indicate that a functional PfATG8 conjugating system is present at the proteomic level and highlight the multiple facets of this pathway in the parasite's infectious cycle progression.

Discussion

The data presented in this study provide a basic understanding of the role of autophagy in the human malaria parasite. Our in silico, cellular, and molecular approaches demonstrate that the canonical autophagy pathway has become modified in *P. falciparum*. Similar to *T. gondii*, *P. falciparum* encodes homologs for only a subset of yeast ATG proteins.[6,7] Upstream kinases involved in detection of nutrient limitation and induction of autophagy are absent. *P. falciparum* is an intracellular parasite residing inside the red blood cell where hemoglobin, its primary nutritional source, is abundant. The parasite may have lost genes required for the nutrient-dependent induction of autophagy, as seen in other systems.[39] This was further confirmed by our observation that autophagy cannot be induced by mild nutrient starvation, or by specific inhibitors of key upstream kinase proteins in the pathway that are involved in regulation in other organisms. Our results are in agreement with a recent study that showed that *P. falciparum* enters a state of hibernation in isoleucine-free medium.[26] Effector proteins that initiate the autophagy pathway in the human malaria parasite remain unknown.

On the contrary, most downstream proteins involved in autophagy were detected in *P. falciparum* and appear to be functional. PfATG proteins involved in autophagosome formation, retrieval, and vesicle breakdown were clearly identified. From the 12 *ATG* genes uncovered from our HMM search, our proteomic analysis identified 7 PfATG proteins, although PfATG2, PfATG5, PfATG6, and PfATG18 were detected at low abundance levels. Proteins of the ATG8 conjugation system (PfATG7, PfATG8, and 2 isoforms of PfATG3) were significantly enriched in the GFP-ATG8 pull-downs, with the exception of PfATG4. Our gel-free mass spectrometry analysis identified the E2-like PfATG3, validating previous reports of a structural characterization of PfATG8-PfATG3 interaction.[40] The role of PfATG4 in priming PfATG8 for PE lipidation remains uncertain. PfATG8 was primarily found conjugated to PE, and proteolytic cleavage by PfAtg4 may not be required for lipidation since PfATG8's C-terminal residue is a glycine. A recent report in *T. gondii* demonstrated that TgATG4 recycles membrane-bound TgATG8,[41] but further investigation will be required to determine the exact role of PfATG4 in recycling PfATG8 from membranes in *Plasmodium*.

In addition to the detection of PfATG8 localizing with the apicoplast[11,12] and its possible involvement in apicoplast biogenesis, we report for the first time the presence of PfATG8-coated vesicles throughout the entire asexual and sexual erythrocytic cycle. Surprisingly, PfATG8 vesicles were also observed within the host RBC. Mature erythrocytes are denucleated and lack proteins involved in vesicle traffic. In order for parasites to transport parasite proteins to the host RBC membrane, parasites have expanded the classical secretory pathway by exporting machinery into the RBC that controls vesicle-mediated traffic.[42] Currently we can only speculate that PfATG8 decorated vesicles in the RBC cytosol are part of the *P. falciparum* exported secretory system. Recently, exosome-like vesicles containing nuclear material were found to be mediators of intercellular communication between parasites.[43] Interestingly, our GO analysis of PfATG8-associated proteins revealed enrichment for the nucleus and nuclear envelope. It is unknown what the contents of PfATG8 vesicles are and if these structures are transported to Maurer's clefts where cargo can be stored for export to the RBC membrane.[44]

Over the years, details of protein trafficking to the apicoplast have remained ambiguous.[14,22,45,46] Apicoplast proteins derived from nuclear-encoded genes utilize a bipartite N-terminal signal peptide to enter the secretory pathway and a transit peptide for apicoplast import.[22,45] The 2 outer membranes of the apicoplast are ER-related.[47] Similarly, the phagophore may also derive from the ER membrane.[48-50] It is therefore possible that these 2 pathways could interact with each other. In apicoplast-minus parasites, PfATG8 localized with vesicles that contain apicoplast-targeted proteins, which suggests an alternative form of bulk protein trafficking to the apicoplast. Further examination into PfATG8 cargo proteins will be necessary to determine the role of PfATG8 and the autophagy machinery's involvement in apicoplast biogenesis.

Interestingly, known inhibitors of the autophagy pathway and parasite development seem to interfere with apicoplast biogenesis. The branch-like structure of the apicoplast observed during the schizont stage was destroyed into multiple foci in both apicoplast-minus parasites and cultures treated with lysosomotropic agents. Both chloroquine and bafilomycin A$_1$ cause vacuolar deacidification and inhibit fusion of autophagosomes with lysosomes. Bafilomycin A$_1$ also blocks transport within the endocytic pathway,[51] but this is the first report of bafilomycin A$_1$ blocking transport to a plastid organelle. Chloroquine is an antimalarial that accumulates in the digestive phagolysosome and inhibits the formation of hemozoin, the byproduct of hemoglobin catabolism.[52] In human fibroblasts, chloroquine also raises intralysosomal pH and disrupts the intracellular pathway for newly synthesized acid hydrolases and uptake by pinocytosis.[53] Reports of cytoplasmic vacuolization, similar to autophagy-associated cell death, have been observed in parasites after chloroquine treatment, but whether or not unicellular protists undergo apoptosis remains ambiguous.[28] Our lysosomotropic drug-treated parasites displayed an accumulation of PfATG8 vesicles and apicoplast fragmentation, which could be interpreted as either cytoplasmic vacuolization or an inhibition of vesicle fusion. In comparison, incubation with the antimalarial artemisinin did not induce autophagy-associated cell death or vacuolization. Further investigations will be needed to determine whether these lysosomotropic agents inhibit fusion with the apicoplast or cause apicoplast fragmentation by vacuolization.

While the asexual stage of the erythrocytic cycle does not last for more than 48 h, the differentiation into gametocytes can take up to 2 weeks.[54] During this time, the parasite resides within the same red blood cell and will need to recycle its proteins in order to survive. The abundance and atypical localization of PfATG8 in gametocytes suggests that autophagy indeed plays an important role in protein turnover and parasite survival. It has been previously reported that the autophagy pathway degrades unnecessary organelles, such as micronemes, during sporozoite metamorphosis into merozoites in the liver stage.[10] Our data show that localization of PfATG8 remains on the apicoplast, but there is an increase in autophagosomes during gametocytogenesis. Considering the apparent role of PfATG8 in gametocyte development, the observation that harsh nutrient starvation induced gametocytogenesis within 48 h without reinvasion of a new erythrocyte may be indicative of a specialized role of autophagy in cell differentiation. Possibly, a delayed or modified form of autophagy induction could trigger differentiation into the sexual stage in *P. falciparum*. Further studies into this process are required to determine the developmental cues necessary for gametocytogenesis.

Collectively, this study presents the critical role of a modified autophagy pathway in the human malaria parasite. PfATG8 has evolved to participate in multiple functions including, but not limited to, cell differentiation, protein turnover, apicoplast biogenesis, and partitioning into daughter cells. While macroautophagy is the best-characterized type of autophagy, our proteomic approach validates the importance of this pathway, but suggests that ribophagy and piecemeal microautophagy of the nucleus may also occur in *P. falciparum*, although additional experiments will be necessary to validate these findings. A detailed understanding of the molecular mechanisms regulating this pathway throughout the human malaria parasite life cycle will not only increase our knowledge of parasite biology, but will most likely uncover novel antimalarial strategies.

Materials and Methods

P. falciparum parasite culture

The following reagents were obtained through the MR4 as part of the BEI Resources Repository, NIAID, NIH: *Plasmodium falciparum* 3D7, MRA-102, deposited by DJ Carucci; Dd2, MRA-156, deposited by TE Wellems; D10 ACP(leader)-GFP, MRA-568, deposited by AF Cowman; D10 ACP(transit)-GFP, MRA-569, deposited by AF Cowman; W2, MRA-157, deposited by DE Kyle; 3D7HT-GFP, MRA-1029, deposited by A Talman and R Sinden; and NF54, MRA-1000, deposited by M Dowler, Walter Reed Army Institute of Research. *P. falciparum* strains were cultured in human O⁺ erythrocytes as previously described.[55] The D10 ACP-GFP transfectant strain was supplemented with 100 nM pyrimethamine (Sigma-Aldrich, P7771).[56] Drug-treated parasites were cultured in the presence of final concentrations of 25 μM artemisinin (Sigma-Aldrich, 361593) and 100 nM chloroquine (Sigma-Aldrich, C6628). Parasites were visualized by fixing thin smears of cultures in methanol for

1 min at room temperature then staining with Modified Giemsa Stain (Sigma-Aldrich, GS128).

HMM search of autophagy-related Pfam domains

Functional Pfam domains found in *ATG* gene-encoded proteins were examined in 11 genomes: *P. falciparum* (release version 8.1), *P. vivax* (release version 8.1), *P. knowlesi* (release version 8.1), *P. yoelii* (release version 8.1), *P. chabaudi* (release version 8.1), *P. berghei* (release version 8.0), *T. gondii* (release version 7.1), *Cryptosporidium hominis* (release version 4.5), *C. parvum* (release version 4.5), *Saccharomyces cerevisiae,* and *Homo sapiens.* The Pfam HMM profiles were downloaded at http://pfam.janelia.org from their Pfam_ls HMM library version 26.0. Additional information regarding Pfam accession numbers are given in **Table S5**. HMM searches were performed, as previously described, in a series of threshold E values, increasing stringency from E value < 0.5 to E value < 0.05 (data not shown).[15] An E value of 0.05 gave the most consistent results when compared with previously published results.

Generation of PfATG8 antibody

PfATG8 was amplified from cDNA using primers forward: CAA<u>TCTAGAC CCGGG</u>AATAA TTTTGTTTAA CTTTAAGAAG and reverse: CAA<u>GGATCCC CATGG</u>GGGTA TAGGGGACAT ACCGCTGC, bearing the restriction enzyme sites XbaI/XmaI and BamHI/NcoI, respectively (underlined). The fragment was inserted into the pGS21a plasmid vector (GenScript, SD0121) using the XbaI and BamHI restriction sites. PfATG8-His$_{6x}$ recombinant protein was expressed in arctic bacterial cells, pulled down using Ni-NTA agarose beads (Qiagen, 30210), and then purified and concentrated by 10- and 30-kDa size exclusion centrifugation (Millipore, UFC901008, UFC903008). Anti-PfATG8 antisera were raised in rabbits and were then purified using protein A/G (Thermo Fisher Scientific, Pierce Custom Antibody Service).

Cloning of *P. falciparum* GFP-fused ATG8

The DNA corresponding to the *P. falciparum ATG8* ortholog (PF3D7_1019900; former ID: PF10_0193) was obtained by PCR from cDNA using primers forward: TCCC<u>CCCGGG</u> ATGCCATCGC TTAAAGACG and reverse: ACGC<u>GTCGAC CTGCAG</u>TTAT CCTAGACAAC TCTCACAAC, bearing the restriction enzyme sites XmaI and SalI/PstI, respectively (underlined). The fragment was cloned into the pCC-1 vector using the XmaI and SalI restriction sites. GFP was then amplified from the pARL/GFP vector (Courtesy of Dr Jude Przyboski, Philipps-Universitat, Marburg, Germany) using the primers forward: CCTG<u>CTCGAG</u> ATGAGTAAAG GAGAAGAACT and reverse: TCCC<u>CCCGGG</u> TTGTATAGTT CATCCATGCC, bearing the restriction enzyme sites XhoI and XmaI, respectively (underlined). The fragment was cloned into the N terminus of the pCC-1/*PfATG8* vector to make pCC-1/GFP-*PfATG8*. Using the primers forward: CAGG<u>CTCGAG</u> <u>ACTAGT</u>ATGA GTAAAGGAGA AGAACT and reverse: GGTC<u>ACCGGT CCCGGGGTCG AC</u>TTATCCTA GACAACTCTC AC, bearing the restriction enzyme sites XhoI/SpeI and AgeI/XmaI/SalI, respectively (underlined), the GFP-PfATG8 fragment was amplified and inserted into the pARL vector using XhoI and AgeI restriction sites. The plasmid pARL/GFP-*PfATG8* was then used

for transient expression of N-terminally GFP-tagged ATG8 in *P. falciparum*. All restriction enzymes used were from New England Biolabs.

Generation of GFP-PfATG8 transient expressing *P. falciparum* cell lines

Parasite transfection was performed as previously described.[57] 3D7 parasite cultures were synchronized with 5% sorbitol and ring stage parasites were used for electroporation with 40 to 50 μg of plasmid DNA. Each electroporation was performed in a 0.2 cm cuvette (Bio-Rad, 165-2086), with time constants ranging from 11–14 ms. The following day, mature parasites were separated by magnetic purification and uninfected RBCs were electroporated with 40 to 50 μg of plasmid DNA. All electroporations were pooled and 50 μl of fresh RBC were added to the culture. The transfected cultures were supplemented with 5 nM WR99210 (Courtesy of Jacobus Pharmaceuticals) for drug selection.[56]

Subcellular fractionation

Parasite subcellular fractions were generated as previously described.[58] Parasites were extracted from red blood cells using 0.15% saponin (Acros, 41923-1000) in PBS (Thermo Fisher Scientific, BP399-1 [11.9 mM phosphate, 137 mM NaCl, 2.7 mM KCl]) on ice for 10 min, followed by 3 ice-cold PBS washes. Parasite pellet fractions were incubated with cytoplasmic lysis buffer (0.65% Igepal [Sigma-Aldrich, I8896], 10 mM TRIS-HCl, pH 7.5, 150 mM NaCl, 1 mM EDTA, 1 mM EGTA, 2 mM AEBSF [Thermo Fisher Scientific, BP63550], 1× Roche protease inhibitor tablet [04693159001]) for 5 min followed by centrifugation at 2,000 rpm for 10 min. The supernatant fraction containing cytoplasmic proteins was removed, samples were washed with PBS, and then subsequently incubated with nuclear lysis buffer (10 mM HEPES, pH 7.9, 0.1 mM EGTA, 0.1 mM EDTA, 1.5 mM $MgCl_2$, 420 mM NaCl, 0.5 mM DTT, 25% glycerol, 2 mM PMSF, 1× Roche protease inhibitor tablet) for 20 min, followed by centrifugation at 6,000 rpm for 10 min. The supernatant fraction containing nuclear proteins was removed, samples were washed with PBS, and then incubated with solubilization lysis buffer (2% Triton X-100, 50 mM TRIS-HCl, pH 7.5, 1 mM EDTA, 1 mM EGTA, 2 mM PMSF, 1× Roche protease inhibitor tablet) for 30 min and were then pelleted at 13,000 rpm for 10 min.[59] The supernatant fraction containing membrane proteins was collected. Protein concentration of samples was determined by the Bradford method.[20] Equal amounts of protein from each fraction were loaded into a 16.5% Tris-Tricine gel, transferred to a PVDF membrane (Bio-Rad, 162-0177), and the membrane was stained with Ponceau S as a loading control before western blot analysis.[60] Verification of fractionation was done with the D10-ACP (transit) cell line, which expresses GFP in the cytoplasm, and fractions were immunoblotted with antibodies to GFP (Abcam, ab290) and histone H3 (Abcam, ab1791) to confirm their presence in the cytosolic and nuclear fractions, respectively.

Western blot analysis

Parasite cultures were incubated in lysis buffer (1% Triton X-100, 50 mM TRIS-HCl, pH 7.5, 1 mM EDTA, 1 mM EGTA, 2 mM PMSF, 1× Roche protease inhibitor tablet) for 30 min on ice and then mechanically lysed by needle and syringe. Samples were then centrifuged at 10,000 rpm for 15 min and the supernatant fraction was removed. Equal amounts of protein, 10 μg, were used for immunoblotting. Regular protein separations were performed using 16.5% Tris-Tricine SDS-PAGE gels (Bio-Rad, 456-3064). Primary antibodies anti-PfATG8 (Thermo Fisher Scientific, Pierce Custom Antibody Service) and anti-GFP were diluted 1:1,500 and 1:3,500, respectively. Secondary antibody goat anti-rabbit IgG HRP conjugate (Bio-Rad, 170-5046) was incubated at a dilution of 1:25,000.

Gametocyte induction

Gametocytes were induced in the NF54, D10 ACP-GFP, and GFP-PfATG8 cell lines following a protocol adapted from Ifediba and Vanderberg.[61] Parasites were synchronized by 5% sorbitol lysis and diluted the following day into 75-cm^2 flasks to reach 0.5% parasitemia at a hematocrit of 8.3% (total volume of 15 ml). Cultures were stressed for 3 d by daily replacement of 10 ml of culture medium. Cultures with 5–10% parasitemia were then induced by increasing the medium to a final volume of 25 ml per flask. For the next 5 d, cultures were maintained by removing 10 ml of medium and adding 10 ml of fresh medium supplemented with 50 mM N-acetyl glucosamine (Alfa Aesar, AAAA13047) to extinguish asexual parasites, followed by feeding with regular medium.

Fluorescence microscopy

P. falciparum parasites were permeabilized with 0.015% saponin, fixed with 4% paraformaldehyde, and blocked with IFA buffer (2% BSA, 0.05% Tween-20, 100 mM glycine, 3 mM EDTA, 150 mM NaCl, 1× PBS). Cells were incubated with anti-PfATG8 antibody (Thermo Fisher Scientific, Pierce Custom Antibody Service; 1:400) followed by anti-rabbit DyLight 550 (abcam ab98489; 1:500). DAPI (Invitrogen, D21490) was included in a wash at a final concentration of 5 μg/ml. Images were acquired using the Olympus BX40 epifluorescence microscope or the Leica SP5 confocal microscope.

Generation of apicoplast-minus *P. falciparum*

Following a similar protocol described by Yeh and DeRisi,[23] parasite cultures were synchronized using 5% sorbitol and ring-stage parasites at 3% parasitemia were grown in 6-well plates (Costar, 3506). The antibiotic chloramphenicol (Sigma-Aldrich, C1919) was added to a final concentration of 100 μM followed by incubation for 48 h. After parasites reinvaded red blood cells, IPP (Isoprenoids LC, IPP001Li) was added to a final concentration of 200 μM to rescue apicoplast-minus parasites. Parasites were grown for an additional generation before sampling cultures for immunofluorescence assays.

P. falciparum starvation

P. falciparum cultures were synchronized by 5% sorbitol. Early and late stage parasites were grown for 6, 24, and 72 h in serum-free complete medium or in starvation medium (0.043 mg/ml gentamicin [GIBCO, 15710-064], 38.5 mM HEPES, 0.18% sodium bicarbonate, 0.003 mM NaOH in RPMI 1640 without L-glutamine and Phenol Red [Corning, 17-105]). Regular media changes were performed every 24 h to remove metabolic waste.

SYBR Green I-based fluorescence assay

Bafilomycin A_1 (LC Laboratories, B-1080) was diluted to 10 μM and serially diluted by thirds into clear bottom 96-well plates (Costar, 3904). *P. falciparum* cultures were added at a

2.5% hematocrit with a 1% parasitemia to 96-well plates and incubated for 72 h at 37 °C. Plates were frozen at –80 °C overnight. Lysis buffer (20 mM TRIS-HCl, 5 mM EDTA, 0.008% saponin, 0.08% Triton X-100, and 0.2 μl/ml SYBR Green I dye (Invitrogen, S7585) was added to thawed plates and incubated at 37 °C. The plates were read using the Spectra Max Gemini EM reader (Molecular Devices). Data were then analyzed with SoftMax Pro v5 (Molecular Devices Software, Inc.).[62]

Immunoprecipitation

The parasite cell lines 3D7, GFP-PfATG8, and HT-GFP were synchronized with 5% sorbitol. To enrich for ATG8 vesicles, samples were incubated with 75 nM of bafilomycin A_1 for 3 h before harvest. Parasites with or without bafilomycin A_1 treatment were extracted from red blood cells using 0.15% saponin. Approximately 2×10^{10} cells (1 ml of parasite pellets) were homogenized by needle and syringe in a total volume of 3.5 ml of lysis buffer [50 mM TRIS-HCl, pH 7.5, 150 mM NaCl, 5 mM EDTA, 1 mM PMSF, 1% Triton X-100, 5 μM E-64 (AG Scientific, Inc., E-2030), Roche complete EDTA-free protease inhibitor cocktail]. Lysates were centrifuged at 13,000 rpm for 10 min and the supernatant fraction was transferred to a clean tube. The supernatant fraction was precleared with PureProteome protein G magnetic beads (Millipore, LSKMAGG02) for 1.5 h. Precleared beads were removed and either anti-PfATG8 or anti-GFP (Abcam, ab290) antibodies were incubated for 6 h at 4 μg/ml before fresh beads were added for 30 min. Our custom anti-PfATG8 antibody was found to not efficiently precipitate endogenous PfATG8 (samples immunoprecipitated by the anti-ATG8 antibody were analyzed by MudPIT; however, the endogenous ATG8 bait [PF3D7_1019900] was either detected with, at best, a couple of peptides and less than 5 spectral counts, or not detected at all [data not shown]). Resin-containing immune complexes were washed twice for each buffer with wash buffers A (1% NP40 [BDH Laboratory Supplies, 56009-2L], 1 mM EDTA, 1% BSA [Invitrogen, 15561-020] in PBS), B (buffer A plus 0.5 M NaCl), C (1% NP40, 1 mM EDTA in PBS), and D (1 mM EDTA in PBS) 2 min, followed by magnetic bead capture. Proteins were first eluted with 0.1 M glycine, pH 2.8 and neutralized with 100 mM TRIS-HCl, pH 8.0, followed by a second elution using the same solution, a third elution using 10% 1,4-dioxane (Thermo Fisher Scientific, D111-500), and a fourth elution with elution buffer (50 mM TRIS-HCl, pH 6.8, 100 mM DTT, 2% SDS) for 40 min at 65 °C. Eluates were pooled and precipitated with 20% trichloroacetic acid (TCA). The resulting pellet fraction was washed once with 10% TCA and 4 times with cold acetone. As a control for the GFP-immunoprecipitation, 2 independent batches of unsynchronized 3D7 cells expressing HT-GFP were prepared in parallel to synchronized 3D7 cells expressing GFP-ATG8 and subjected to the same GFP-affinity purification protocol. As a control to overexpressing GFP-ATG8 in cells, 2 independent replicates of 3D7 unsynchronized cells expressing GFP-ATG8 were also subjected to immunoprecipitation using a nonspecific antibody.

MudPIT analysis of immunoprecipitated proteins

TCA-precipitated proteins were solubilized in 100 mM TRIS-HCl, pH 8.5, 8 M Urea, 5 mM Tris(2-carboxylethyl)-phosphine hydrochloride (TRIS-HCl, Sigma-Aldrich, T3253; urea, Sigma-Aldrich, U1250; TCEP-HCl, Pierce, 20490) before chloroacetamide (Sigma-Aldrich, C0267) was added to a final concentration of 10 mM. Endoproteinase Lys-C (Roche Applied Science, 11047825001) was used at 1:100 w/w to digest proteins overnight at 37 °C. Samples were then brought to a final concentration of 2 M urea with 100 mM TRIS-HCl, pH 8.5 and 2 mM $CaCl_2$ (VWR Scientific Products Inc., EM3000) before adding trypsin (VWR Scientific Products Inc., EM3000) (Promega, V5111) at 1:100 w/w for a second overnight digestion at 37 °C. Formic acid (VWR Scientific Products Inc., JT0129-1) was added to a final concentration of 5% before samples were loaded onto a split-triple-phase fused-silica microcapillary column (Deactivated fused silica tubing, 0.250 × 0.360 mm: Agilent Technologies, 160-2255-30; Deactivated fused silica tubing, 0.100 × 0.360 mm: Molex Connector Corp, 2000023),[63] and placed in-line with a quaternary agilent 1100/1200 series HPLC (ThermoScientific) LTQ ion trap mass spectrometer equipped with a custom-made nanospray ionization source. Full MS spectra were recorded on the peptides over a 400 to 1,600 m/z range, followed by 5 tandem mass (MS/MS) events sequentially generated in a data-dependent manner on the first to fifth most intense ions selected from the full MS spectrum (at 35% collision energy).[64] The dynamic exclusion was enabled for 120 s. A total of 3 technical replicates were acquired for each of the 4 types of samples analyzed (early trophozoite with and without bafilomycin A_1 treatment and late schizont with or without bafilomycin A_1 treatment). GFP-immunoprecipitations from 2 batches of asynchronized 3D7-HT-GFP cells and immunoprecipitations in the absence of an antibody from 2 batches of asynchronized GFP-PfATG8 3D7 cells were also analyzed as negative controls.

Proteomics data analysis

The MS/MS data sets were searched using SEQUEST against a protein database consisting of 5,538 *P. falciparum* (PlasmoDB rerelease 9.1) and 34,521 *H. sapiens* (NCBI 2012-08-27 release) proteins, complemented with 177 sequences from usual contaminants (human keratins, IgGs, proteolytic enzymes). To estimate false-positive discovery rates (FDR), each sequence was randomized (keeping amino acid composition and length the same) and the resulting "shuffled" sequences were added to the "normal" database (doubling its size) and searched at the same time. The GFP-PfATG8 sequence was added to this database. To limit the number of false-positive "shuffled" peptides passing the selection criteria, the filtering criteria were strict, notably enforcing that both peptide ends matched the enzyme used for the digestion. The average protein FDR was 2.6%, peptide FDR was 1.06%, and the spectral FDR was 0.40%.[65]

To address the question of whether any differences were observable between the samples and the controls, we used multiple criteria to filter proteins associating with ATG8. First, proteins had to be detected reproducibly in at least one of the 4 types of samples analyzed, i.e., present in at least 2 of the 3 replicates acquired per sample type. Next, proteins were either not detected in controls or with a 5-fold increase based on normalized spectral counts. We narrowed down the list of significant proteins further by requiring that the proteins be at least present

in 4 out of the 12 analyses. Finally, for proteins passing these criteria but detected in the controls, we calculated the fold changes between the respective purifications using a z-statistics-based statistical framework (update QSpec) for the significance analysis of differential expression.[32] The z-score was calculated using the web submission at http://www.nesvilab.org/qspec.php/. The spectral counts and the length of each protein were used as input for the QSpec software. We only kept proteins with the additional z-score filter of > 1.7.

Gene ontology analysis

Enrichment of gene ontology (GO) terms within each sample was analyzed using the software package "topGO" (written in R and maintained by the BioConductor project).[66] For each GO domain (i.e., cellular component, biological process or molecular function), we compared the proteins identified by MudPIT to the full proteome of *P. falciparum* using the "classic" algorithm in combination with a Fisher's exact test. In addition, GO enrichment was analyzed among all ATG8-associated proteins identified by MudPIT, irrespective of time point or drug treatment. Gene ontology structures were visualized for GO terms with a *P* value < 0.01 using the R software package "Rgraphviz".[67] To illustrate overlaps in GO terms between the different samples, a Venn diagram was drawn including all GO terms with a *P* value < 0.05 using the R software package "venneuler".[68]

Supplemental Materials

Supplemental materials may be found here:
www.landesbioscience.com/journals/autophagy/article/26743

References

1. World Malaria Report WHOU. 2012. Geneva, Switzerland and New York, USA 2012.
2. Tsukada M, Ohsumi Y. Isolation and characterization of autophagy-defective mutants of *Saccharomyces cerevisiae*. FEBS Lett 1993; 333:169-74; PMID:8224160; http://dx.doi.org/10.1016/0014-5793(93)80398-E
3. Mizushima N, Levine B, Cuervo AM, Klionsky DJ. Autophagy fights disease through cellular self-digestion. Nature 2008; 451:1069-75; PMID:18305538; http://dx.doi.org/10.1038/nature06639
4. Klionsky DJ, Abdalla FC, Abeliovich H, Abraham RT, Acevedo-Arozena A, Adeli K, Agholme L, Agnello M, Agostinis P, Aguirre-Ghiso JA, et al. Guidelines for the use and interpretation of assays for monitoring autophagy. Autophagy 2012; 8:445-544; PMID:22966490; http://dx.doi.org/10.4161/auto.19496
5. Nakatogawa H, Suzuki K, Kamada Y, Ohsumi Y. Dynamics and diversity in autophagy mechanisms: lessons from yeast. Nat Rev Mol Cell Biol 2009; 10:458-67; PMID:19491929; http://dx.doi.org/10.1038/nrm2708
6. Duszenko M, Ginger ML, Brennand A, Gualdrón-López M, Colombo MI, Coombs GH, Coppens I, Jayabalasingham B, Langsley G, de Castro SL, et al. Autophagy in protists. Autophagy 2011; 7:127-58; PMID:20962583; http://dx.doi.org/10.4161/auto.7.2.13310
7. Brennand A, Gualdrón-López M, Coppens I, Rigden DJ, Ginger ML, Michels PA. Autophagy in parasitic protists: unique features and drug targets. Mol Biochem Parasitol 2011; 177:83-99; PMID:21315770; http://dx.doi.org/10.1016/j.molbiopara.2011.02.003
8. Ghosh D, Walton JL, Roepe PD, Sinai AP. Autophagy is a cell death mechanism in Toxoplasma gondii. Cell Microbiol 2012; 14:589-607; PMID:22212386; http://dx.doi.org/10.1111/j.1462-5822.2011.01745.x
9. Besteiro S, Brooks CF, Striepen B, Dubremetz JF. Autophagy protein Atg3 is essential for maintaining mitochondrial integrity and for normal intracellular development of *Toxoplasma gondii* tachyzoites. PLoS Pathog 2011; 7:e1002416; PMID:22144900; http://dx.doi.org/10.1371/journal.ppat.1002416
10. Jayabalasingham B, Bano N, Coppens I. Metamorphosis of the malaria parasite in the liver is associated with organelle clearance. Cell Res 2010; 20:1043-59; PMID:20567259; http://dx.doi.org/10.1038/cr.2010.88

11. Kitamura K, Kishi-Itakura C, Tsuboi T, Sato S, Kita K, Ohta N, Mizushima N. Autophagy-related Atg8 localizes to the apicoplast of the human malaria parasite *Plasmodium falciparum*. PLoS One 2012; 7:e42977; PMID:22900071; http://dx.doi.org/10.1371/journal.pone.0042977
12. Eickel N, Kaiser G, Prado M, Burda PC, Roelli M, Stanway RR, Heussler VT. Features of autophagic cell death in Plasmodium liver-stage parasites. Autophagy 2013; 9:568-80; PMID:23388496; http://dx.doi.org/10.4161/auto.23689
13. van Dooren GG, Marti M, Tonkin CJ, Stimmler LM, Cowman AF, McFadden GI. Development of the endoplasmic reticulum, mitochondrion and apicoplast during the asexual life cycle of Plasmodium falciparum. Mol Microbiol 2005; 57:405-19; PMID:15978074; http://dx.doi.org/10.1111/j.1365-2958.2005.04699.x
14. van Dooren GG, Waller RF, Joiner KA, Roos DS, McFadden GI. Traffic jams: protein transport in *Plasmodium falciparum*. Parasitol Today 2000; 16:421-7; PMID:11006473; http://dx.doi.org/10.1016/S0169-4758(00)01792-0
15. Ponts N, Yang J, Chung DW, Prudhomme J, Girke T, Horrocks P, Le Roch KG. Deciphering the ubiquitin-mediated pathway in apicomplexan parasites: a potential strategy to interfere with parasite virulence. PLoS One 2008; 3:e2386; PMID:18545708; http://dx.doi.org/10.1371/journal.pone.0002386
16. Coppens I. Metamorphoses of malaria: the role of autophagy in parasite differentiation. Essays Biochem 2011; 51:127-36; PMID:22023446
17. Lang T, Schaeffeler E, Bernreuther D, Bredschneider M, Wolf DH, Thumm M. Aut2p and Aut7p, two novel microtubule-associated proteins are essential for delivery of autophagic vesicles to the vacuole. EMBO J 1998; 17:3597-607; PMID:9649430; http://dx.doi.org/10.1093/emboj/17.13.3597
18. Teter SA, Eggerton KP, Scott SV, Kim J, Fischer AM, Klionsky DJ. Degradation of lipid vesicles in the yeast vacuole requires function of Cvt17, a putative lipase. J Biol Chem 2001; 276:2083-7; PMID:11085977
19. Nakatogawa H, Ichimura Y, Ohsumi Y. Atg8, a ubiquitin-like protein required for autophagosome formation, mediates membrane tethering and hemifusion. Cell 2007; 130:165-78; PMID:17632063; http://dx.doi.org/10.1016/j.cell.2007.05.021

20. Bradford MM. A rapid and sensitive method for the quantitation of microgram quantities of protein utilizing the principle of protein-dye binding. Anal Biochem 1976; 72:248-54; PMID:942051; http://dx.doi.org/10.1016/0003-2697(76)90527-3
21. Tomlins AM, Ben-Rached F, Williams RA, Proto WR, Coppens I, Ruch U, Gilberger TW, Coombs GH, Mottram JC, Müller S, et al. *Plasmodium falciparum* ATG8 implicated in both autophagy and apicoplast formation. Autophagy 2013; 9:1540-52; PMID:24025672; http://dx.doi.org/10.4161/auto.25832
22. Waller RF, Reed MB, Cowman AF, McFadden GI. Protein trafficking to the plastid of *Plasmodium falciparum* is via the secretory pathway. EMBO J 2000; 19:1794-802; PMID:10775264; http://dx.doi.org/10.1093/emboj/19.8.1794
23. Yeh E, DeRisi JL. Chemical rescue of malaria parasites lacking an apicoplast defines organelle function in blood-stage *Plasmodium falciparum*. PLoS Biol 2011; 9:e1001138; PMID:21912516; http://dx.doi.org/10.1371/journal.pbio.1001138
24. Baker DA. Malaria gametocytogenesis. Mol Biochem Parasitol 2010; 172:57-65; PMID:20381542; http://dx.doi.org/10.1016/j.molbiopara.2010.03.019
25. Okamoto N, Spurck TP, Goodman CD, McFadden GI. Apicoplast and mitochondrion in gametocytogenesis of *Plasmodium falciparum*. Eukaryot Cell 2009; 8:128-32; PMID:18996983; http://dx.doi.org/10.1128/EC.00267-08
26. Babbitt SE, Altenhofen L, Cobbold SA, Istvan ES, Fennell C, Doerig C, Llinás M, Goldberg DE. *Plasmodium falciparum* responds to amino acid starvation by entering into a hibernatory state. Proc Natl Acad Sci U S A 2012; 109:E3278-87; PMID:23112171; http://dx.doi.org/10.1073/pnas.1209823109
27. Yamamoto A, Tagawa Y, Yoshimori T, Moriyama Y, Masaki R, Tashiro Y. Bafilomycin A1 prevents maturation of autophagic vacuoles by inhibiting fusion between autophagosomes and lysosomes in rat hepatoma cell line, H-4-II-E cells. Cell Struct Funct 1998; 23:33-42; PMID:9639028; http://dx.doi.org/10.1247/csf.23.33
28. Totino PR, Daniel-Ribeiro CT, Corte-Real S, de Fátima Ferreira-da-Cruz M. *Plasmodium falciparum*: erythrocytic stages die by autophagic-like cell death under drug pressure. Exp Parasitol 2008; 118:478-86; PMID:18226811; http://dx.doi.org/10.1016/j.exppara.2007.10.017

29. Dondorp AM, Nosten F, Yi P, Das D, Phyo AP, Tarning J, Lwin KM, Ariey F, Hanpithakpong W, Lee SJ, et al. Artemisinin resistance in *Plasmodium falciparum* malaria. N Engl J Med 2009; 361:455-67; PMID:19641202; http://dx.doi.org/10.1056/NEJMoa0808859

30. Washburn MP, Wolters D, Yates JR 3rd. Large-scale analysis of the yeast proteome by multidimensional protein identification technology. Nat Biotechnol 2001; 19:242-7; PMID:11231557; http://dx.doi.org/10.1038/85686

31. Talman AM, Blagborough AM, Sinden RE. A *Plasmodium falciparum* strain expressing GFP throughout the parasite's life-cycle. PLoS One 2010; 5:e9156; PMID:20161781; http://dx.doi.org/10.1371/journal.pone.0009156

32. Choi H, Fermin D, Nesvizhskii AI. Significance analysis of spectral count data in label-free shotgun proteomics. Mol Cell Proteomics 2008; 7:2373-85; PMID:18644780; http://dx.doi.org/10.1074/mcp.M800203-MCP200

33. Behrends C, Sowa ME, Gygi SP, Harper JW. Network organization of the human autophagy system. Nature 2010; 466:68-76; PMID:20562859; http://dx.doi.org/10.1038/nature09204

34. Kabeya Y, Kamada Y, Baba M, Takikawa H, Sasaki M, Ohsumi Y. Atg17 functions in cooperation with Atg1 and Atg13 in yeast autophagy. Mol Biol Cell 2005; 16:2544-53; PMID:15743910; http://dx.doi.org/10.1091/mbc.E04-08-0669

35. Dawaliby R, Mayer A. Microautophagy of the nucleus coincides with a vacuolar diffusion barrier at nuclear-vacuolar junctions. Mol Biol Cell 2010; 21:4173-83; PMID:20943953; http://dx.doi.org/10.1091/mbc.E09-09-0782

36. Mijaljica D, Prescott M, Devenish RJ. The intricacy of nuclear membrane dynamics during nucleophagy. Nucleus 2010; 1:213-23; PMID:21327066; http://dx.doi.org/10.4161/nucl.1.3.11738

37. Kraft C, Deplazes A, Sohrmann M, Peter M. Mature ribosomes are selectively degraded upon starvation by an autophagy pathway requiring the Ubp3p/Bre5p ubiquitin protease. Nat Cell Biol 2008; 10:602-10; PMID:18391941; http://dx.doi.org/10.1038/ncb1723

38. Ossareh-Nazari B, Bonizec M, Cohen M, Dokudovskaya S, Delalande F, Schaeffer C, Van Dorsselaer A, Dargemont C. Cdc48 and Ufd3, new partners of the ubiquitin protease Ubp3, are required for ribophagy. EMBO Rep 2010; 11:548-54; PMID:20508643; http://dx.doi.org/10.1038/embor.2010.74

39. Kamada Y, Funakoshi T, Shintani T, Nagano K, Ohsumi M, Ohsumi Y. Tor-mediated induction of autophagy via an Apg1 protein kinase complex. J Cell Biol 2000; 150:1507-13; PMID:10995454; http://dx.doi.org/10.1083/jcb.150.6.1507

40. Hain AU, Weltzer RR, Hammond H, Jayabalasingham B, Dinglasan RR, Graham DR, Colquhoun DR, Coppens I, Bosch J. Structural characterization and inhibition of the Plasmodium Atg8-Atg3 interaction. J Struct Biol 2012; 180:551-62; PMID:22982544; http://dx.doi.org/10.1016/j.jsb.2012.09.001

41. Kong-Hap MA, Mouammine A, Daher W, Berry L, Lebrun M, Dubremetz JF, Besteiro S. Regulation of ATG8 membrane association by ATG4 in the parasitic protist *Toxoplasma gondii*. Autophagy 2013; 9:1334-48; PMID:23748741; http://dx.doi.org/10.4161/auto.25189

42. Hanssen E, McMillan PJ, Tilley L. Cellular architecture of *Plasmodium falciparum*-infected erythrocytes. Int J Parasitol 2010; 40:1127-35; PMID:20478310; http://dx.doi.org/10.1016/j.ijpara.2010.04.012

43. Regev-Rudzki N, Wilson DW, Carvalho TG, Sisquella X, Coleman BM, Rug M, Bursac D, Angrisano F, Gee M, Hill AF, et al. Cell-cell communication between malaria-infected red blood cells via exosome-like vesicles. Cell 2013; 153:1120-33; PMID:23683579; http://dx.doi.org/10.1016/j.cell.2013.04.029

44. Przyborski JM, Miller SK, Pfahler JM, Henrich PP, Rohrbach P, Crabb BS, Lanzer M. Trafficking of STEVOR to the Maurer's clefts in Plasmodium falciparum-infected erythrocytes. EMBO J 2005; 24:2306-17; PMID:15961998; http://dx.doi.org/10.1038/sj.emboj.7600720

45. Foth BJ, Ralph SA, Tonkin CJ, Struck NS, Fraunholz M, Roos DS, Cowman AF, McFadden GI. Dissecting apicoplast targeting in the malaria parasite *Plasmodium falciparum*. Science 2003; 299:705-8; PMID:12560551; http://dx.doi.org/10.1126/science.1078599

46. Jackson KE, Pham JS, Kwek M, De Silva NS, Allen SM, Goodman CD, McFadden GI, de Pouplana LR, Ralph SA. Dual targeting of aminoacyl-tRNA synthetases to the apicoplast and cytosol in *Plasmodium falciparum*. Int J Parasitol 2012; 42:177-86; PMID:22222968; http://dx.doi.org/10.1016/j.ijpara.2011.11.008

47. Deponte M, Hoppe HC, Lee MC, Maier AG, Richard D, Rug M, Spielmann T, Przyborski JM. Wherever I may roam: protein and membrane trafficking in *P. falciparum*-infected red blood cells. Mol Biochem Parasitol 2012; 186:95-116; PMID:23043991; http://dx.doi.org/10.1016/j.molbiopara.2012.09.007

48. Axe EL, Walker SA, Manifava M, Chandra P, Roderick HL, Habermann A, Griffiths G, Ktistakis NT. Autophagosome formation from membrane compartments enriched in phosphatidylinositol 3-phosphate and dynamically connected to the endoplasmic reticulum. J Cell Biol 2008; 182:685-701; PMID:18725538; http://dx.doi.org/10.1083/jcb.200803137

49. Hayashi-Nishino M, Fujita N, Noda T, Yamaguchi A, Yoshimori T, Yamamoto A. A subdomain of the endoplasmic reticulum forms a cradle for autophagosome formation. Nat Cell Biol 2009; 11:1433-7; PMID:19898463; http://dx.doi.org/10.1038/ncb1991

50. Ylä-Anttila P, Vihinen H, Jokitalo E, Eskelinen E-L. 3D tomography reveals connections between the phagophore and endoplasmic reticulum. Autophagy 2009; 5:1180-5; PMID:19855179; http://dx.doi.org/10.4161/auto.5.8.10274

51. Klionsky DJ, Elazar Z, Seglen PO, Rubinsztein DC. Does bafilomycin A1 block the fusion of autophagosomes with lysosomes? Autophagy 2008; 4:849-50; PMID:18758232

52. Sullivan DJ Jr., Gluzman IY, Russell DG, Goldberg DE. On the molecular mechanism of chloroquine's antimalarial action. Proc Natl Acad Sci U S A 1996; 93:11865-70; PMID:8876229; http://dx.doi.org/10.1073/pnas.93.21.11865

53. Gonzalez-Noriega A, Grubb JH, Talkad V, Sly WS. Chloroquine inhibits lysosomal enzyme pinocytosis and enhances lysosomal enzyme secretion by impairing receptor recycling. J Cell Biol 1980; 85:839-52; PMID:7190150; http://dx.doi.org/10.1083/jcb.85.3.839

54. Alano P. *Plasmodium falciparum* gametocytes: still many secrets of a hidden life. Mol Microbiol 2007; 66:291-302; PMID:17784927; http://dx.doi.org/10.1111/j.1365-2958.2007.05904.x

55. Trager W, Jensen JB. Human malaria parasites in continuous culture. 1976. J Parasitol 2005; 91:484-6; PMID:16108535; http://dx.doi.org/10.1645/0022-3395(2005)091[0484:HMPICC]2.0.CO;2

56. de Koning-Ward TF, Fidock DA, Thathy V, Menard R, van Spaendonk RM, Waters AP, Janse CJ. The selectable marker human dihydrofolate reductase enables sequential genetic manipulation of the *Plasmodium berghei* genome. Mol Biochem Parasitol 2000; 106:199-212; PMID:10699250; http://dx.doi.org/10.1016/S0166-6851(99)00189-9

57. Wu Y, Sifri CD, Lei HH, Su XZ, Wellems TE. Transfection of Plasmodium falciparum within human red blood cells. Proc Natl Acad Sci U S A 1995; 92:973-7; PMID:7862676; http://dx.doi.org/10.1073/pnas.92.4.973

58. Le Roch KG, Johnson JR, Florens L, Zhou Y, Santrosyan A, Grainger M, Yan SF, Williamson KC, Holder AA, Carucci DJ, et al. Global analysis of transcript and protein levels across the *Plasmodium falciparum* life cycle. Genome Res 2004; 14:2308-18; PMID:15520293; http://dx.doi.org/10.1101/gr.2523904

59. Topolska AE, Lidgett A, Truman D, Fujioka H, Coppel RL. Characterization of a membrane-associated rhoptry protein of *Plasmodium falciparum*. J Biol Chem 2004; 279:4648-56; PMID:14613941; http://dx.doi.org/10.1074/jbc.M307859200

60. Romero-Calvo I, Ocón B, Martínez-Moya P, Suárez MD, Zarzuelo A, Martínez-Augustin O, de Medina FS. Reversible Ponceau staining as a loading control alternative to actin in Western blots. Anal Biochem 2010; 401:318-20; PMID:20206115; http://dx.doi.org/10.1016/j.ab.2010.02.036

61. Ifediba T, Vanderberg JP. Complete in vitro maturation of *Plasmodium falciparum* gametocytes. Nature 1981; 294:364-6; PMID:7031476; http://dx.doi.org/10.1038/294364a0

62. Cervantes S, Stout PE, Prudhomme J, Engel S, Bruton M, Cervantes M, Carter D, Tae-Chang Y, Hay ME, Aalbersberg W, et al. High content live cell imaging for the discovery of new antimalarial marine natural products. BMC Infect Dis 2012; 12:1; PMID:22214291; http://dx.doi.org/10.1186/1471-2334-12-1

63. McDonald WH, Ohi R, Miyamoto DT, Mitchison TJ, Yates JR 3rd. Comparison of three directly coupled HPLC MS/MS strategies for identification of proteins from complex mixtures: single-dimension LC-MS/MS, 2-phase MudPIT, and 3-phase MudPIT. Int J Mass Spectrom 2002; 219:245-51; http://dx.doi.org/10.1016/S1387-3806(02)00563-8

64. Zhang Y, Wen Z, Washburn MP, Florens L. Refinements to label free proteome quantitation: how to deal with peptides shared by multiple proteins. Anal Chem 2010; 82:2272-81; PMID:20166708; http://dx.doi.org/10.1021/ac9023999

65. Ponts N, Saraf A, Chung DW, Harris A, Prudhomme J, Washburn MP, Florens L, Le Roch KG. Unraveling the ubiquitome of the human malaria parasite. J Biol Chem 2011; 286:40320-30; PMID:21930698; http://dx.doi.org/10.1074/jbc.M111.238790

66. Alexa A, Rahnenfuhrer J. topGO: topGO: Enrichment analysis for Gene Ontology 2010

67. Gentry J, Long L, Gentleman R, Falcon S, Hahne F, Sarkar D, et al. Rgraphviz: Provides plotting capabilities for R graph objects

68. Wilkinson L. venneuler: Venn and Euler Diagrams 2011